Vol 17 No 6, June 2008
1674-1056/2008/17(06)/2222-07

Chinese Physics B

© 2008 Chin. Phys. Soc.
and IOP Publishing Ltd

# Electronic structure and optical properties of $LiXH_3$ and $XLiH_3$ ($X =$ Be, B or C)*

San Xiao-Jiao(伞晓娇), He Zhi(何 志), Ma Yan-Ming(马琰铭),
Cui Tian(崔 田)†, Liu Bing-Bing(刘冰冰), and Zou Guang-Tian(邹广田)

*National Laboratory of Superhard Materials, Jilin University, Changchun* 130012, *China*

(Received 9 November 2007; revised manuscript received 25 December 2007)

The equilibrium lattice constant, the cohesive energy and the electronic properties of light metal hydrides $LiXH_3$ and $XLiH_3$ ($X =$ Be, B or C) with perovskite lattice structures have been investigated by using the pseudopotential plane-wave method. Large energy gap of $LiBeH_3$ indicates that it is insulating, but other investigated hydrides are metallic. The pressure-induced metallization of $LiBeH_3$ is found at about 120 GPa, which is attributed to the increase of Be-p electrons with pressure. The electronegativity of the p electrons of $X$ atom is responsible for the metallicity of the investigated $LiXH_3$ hydrides, but the electronegativity of the s electrons of $X$ atom plays an important role in the metallicity of the investigated $XLiH_3$ hydrides. In order to deeply understand the investigated hydrides, their optical properties have also been investigated. The optical absorption of either $LiBeH_3$ or $BeLiH_3$ has a strong peak at about 5 eV, showing that their optical responses are qualitatively similar. It is also found that the optical responses of other investigated hydrides are stronger than those of $LiBeH_3$ and $BeLiH_3$ in lower energy ranges, especially in the case of $CLiH_3$.

**Keywords:** plane-wave method, metal hydrides, electronic structure, optical properties
**PACC:** 7125, 7130

## 1. Introduction

$LiBeH_3$, as a potential high-$T_c$ conventional superconductor, was first investigated by Overhauser[1,2] in 1987. Since then, a large number of theoretical studies of the electronic band structure and density of states have been carried out by using various theoretical approaches and models.[3−8] All of the calculations reveal that $LiBeH_3$ is not metallic with a large band gap. Nonetheless, many problems remain unclear, such as the electronic structure, the physical mechanism of the pressure-induced metallization of $LiBeH_3$ and the differences among the light metal hydrides with similar chemical composition or structure.

$LiBeH_3$ was firstly synthesized in 1968 by Bell and Coates.[9] By analysing their x-ray-diffraction patterns, Overhauser concluded that they had obtained a mixture of two kinds of perovskite '$LiBeH_3$' successfully.[1,2] The first one had a normal perovskite structure ($LiBeH_3$), where the Be was located at the centre site and Li at the corner site, and the second one had the inverse perovskite structure ($BeLiH_3$), where the positions of Be and Li were exchanged. The hydrogen atoms resided at the face centres in both cases. Yu and Lam[6] performed first-principles total-energy and electronic band-structure calculations on '$LiBeH_3$' in 1988. Their results indicated that the normal perovskite mode $LiBeH_3$ was more stable and of a semiconductor with an indirect band gap of about 1.0 eV at ambient pressure, but the inverse perovskite mode $BeLiH_3$ was metallic if its structure consisted of units of the perovskite type. Furthermore, they predicted that the pressure-induced metallization of $LiBeH_3$ could occur at 70 GPa. The recently experimental measurements on Li-Be-H system showed that it could be type-II superconductor under applied pressures.[10]

Many theoretical studies on a LiH system have been carried out by using *ab initio* calculations.[11,12] Other light metal hydrides including $LiBH_3$ and binary intermetallic hydrides such as $MM'H_x$, $MAlH_4$, and $M'(AlH_4)_2$, where $M$and $M'$ denote a light alkali and alkaline-earth metal, respectively, have been

*Project supported by the National Natural Science Foundation of China (Grant Nos 10574053 and 10674053), the 2004 NCET and 2003 EYTP of MOE of China, the National Basic Research Program of China (Grant Nos 2005CB724400 and 2001CB711201), and the Cultivation Fund of the Key Scientific and Technical Innovation Project, China (Grant No 2004-295).
†Corresponding author. E-mail: cuitian@jlu.edu.cn

also studied extensively.[7,8,13] Except LiBH$_3$ behaving as a metal, other hydrides are all insulating. Seel *et al*[7] investigated the electronic structures of LiBeH$_3$ and LiBH$_3$ with the cubic perovskite structures using the Hartree-Fock linear combination of atomic orbitals (LCAO) calculations in 1989. Their results indicated that LiBeH$_3$ was of a semiconductor at ambient pressure, but LiBH$_3$ was metallic. Then, in 1997, Khowash *et al*[8] studied a series of light metal hydrides (LiBeH$_3$, LiMgH$_3$, LiCaH$_3$, NaMgH$_3$, and LiBH$_3$) with the same perovskite lattice structures by using the linear combination of muffin-tin orbital method (LMTO), and their results showed that only LiBH$_3$ was metallic too. In this work, we investigate the electronic and optical properties and the pressure effect on the series hydrides, in order to deeply understand the investigated hydrides.

## 2. Methods

Pseudopotential plane wave (PW) *ab initio* calculations[14] are performed within the framework of density-functional theory (DFT) through the Cambridge Sequential Total Energy Package (CASTEP).[15] The generalized gradient approximation (GGA) with the Perdew–Burke–Ernzerhof (PBE) functionals[16] is employed. The Vanderbilt ultrasoft pseudopotential[17] with an energy cutoff of 400 eV and a 16×16×16 Monkhorst pack grid[18,19] are used in the electronic Brillouin zone integration for all calculations. Before any electronic structure calculation, the cell parameters and the atomic positions within a unit cell are optimized by using BFGS (proposed by Broyden, Fletcher, Goldfarb, and Shannon) minimization algorithm.[20]

## 3. Results and discussion

Our theoretical lattice constants, cohesive energy, bulk modulus, and band gaps of various light metal hydrides at zero pressure, together with the LMTO results[8] and other calculations,[6] are listed in Table 1. Our PW results in the equilibrium lattice constants and bulk modulus are in good agreement with the previously available results. The previous research shows that the hydrogen-related bands in a more electronegative host matrix should lie closer to the Fermi levels in the series of $X$LiH$_3$ and Li$X$H$_3$ hydrides, which makes the hydrides become metallic.[8] So we investigate the electronic structures of LiBH$_3$, LiCH$_3$ with the same structure as LiBeH$_3$, and their inverse perovskite structures BLiH$_3$ and CLiH$_3$ with the same structure as BeLiH$_3$. Table 1 show that other hydrides are metallic except LiBeH$_3$, which are consistent with the results of Khowash *et al*. Our calculated band gap of LiBeH$_3$ is about 1.3 eV, which is in a range of the earlier theoretical results, 0.8–1.6 eV. The lattice parameter decreases with the increase of atomic number $X$ in the two perovskite modes hydrides, separately. The lattice parameter of LiBeH$_3$ is larger than of its inverse perovskite structure BeLiH$_3$, but in the cases of LiBH$_3$and LiCH$_3$, the lattice parameter of the normal perovskite structures is smaller than those of the inverse perovskite structures BLiH$_3$ and CLiH$_3$, respectively. The bond overlap population (BOP) between Li and $X$ atoms is also listed in Table 1. It is found that the BOP increases from LiBeH$_3$ to BeLiH$_3$,

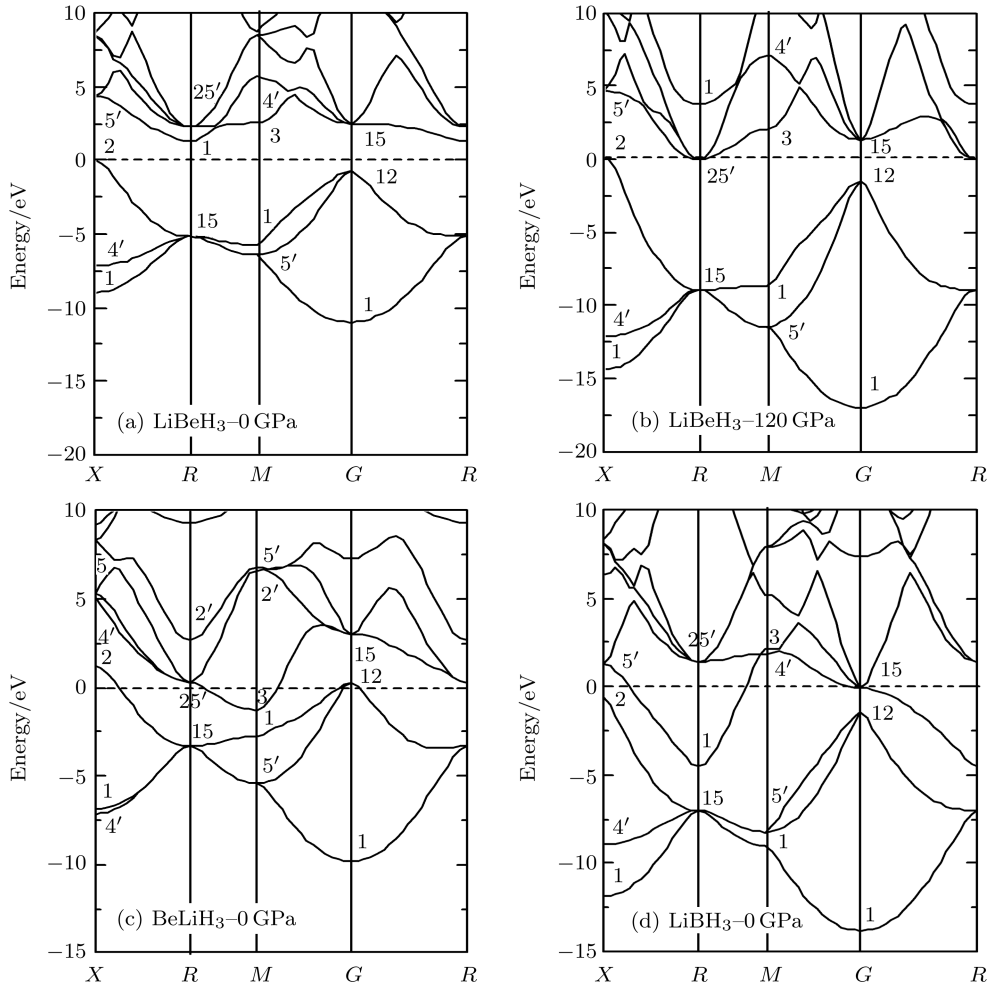
**Table 1.** The calculated equilibrium lattice constant, cohesive energy, bulk modulus, band gap, and bond overlap population between Li and X atoms of the different lightweight metal hydrides under 0 GPa.

| System | $a$/nm | | | Cohesive energy /(eV/atom) | | $B_0$/GPa | | band gap/eV | | | BOP/$\|e\|$ |
|---|---|---|---|---|---|---|---|---|---|---|---|
| | Ref.[8] | Ref.[6] | Ours | Ref.[6] | Ours | Ref.[6] | Ours | Ref.[8] | Ref.[6] | Ours | Ours |
| LiBeH$_3$ | 0.336 | 0.319 | 0.316 | 2.84 | 2.53 | 69.0 | 63.8 | 1.5 | 0.8 | 1.3 | 0.73 |
| LiBH$_3$ | 0.311 | | 0.306 | | 2.81 | | 81.9 | | | | 0.36 |
| LiCH$_3$ | | | 0.293 | | 3.06 | | 118.6 | | | | 0.25 |
| BeLiH$_3$ | | 0.318 | 0.313 | 2.07 | 1.82 | 60.0 | 63.8 | | | | 1.08 |
| BLiH$_3$ | 0.295 | | 0.311 | | 1.81 | | 53.8 | | | | 0.13 |
| CLiH$_3$ | | | 0.310 | | 1.81 | | 122.6 | | | | 0.14 |

but decreases from $LiBH_3$ and $LiCH_3$ to their corresponding inverse structures. This fact in BOP may contribute to the anomalous behaviours in the lattice parameter of these hydrides. Although our calculated cohesive energy is smaller than the result in Ref.[6] due to the using of different pseudopotentials, the relative value among these hydrides is more meaningful. A comparison of cohesive energy between $LiXH_3$ and $XLiH_3$ shows that $LiXH_3$ is more stable than $XLiH_3$. The difference in cohesive energy between $LiBeH_3$ and $BeLiH_3$ is 0.71 eV/atom, which is very close to the value of 0.77 eV/atom in Ref.[6]. In order to understand the properties and the pressure effect on these hydrides, we investigate the band structure, density of states, electronic population, and optical properties at ambient pressure and high pressures.

The band structures of $LiBeH_3$ at 0 GPa and a metallization pressure of 120 GPa are shown in Figs.1(a) and 1(b), and the electronic band structures of $BeLiH_3$, $LiBH_3$, $LiCH_3$, and $CLiH_3$ at 0 GPa are shown in Figs.1(c)–(f), respectively. The bands are labelled according to the notations in Refs.[6, 21].

From Figs.1(a) and 1(b), it is found that the conduction band $R'_{25}$ drops towards the Fermi level and the valence band $X_2$ steps up with the increase of pressure. But the valence band $X_2$ crosses the Fermi level firstly. Except for a small and nearly spherical part around $X_2$, the third band is almost completely filled. The partial density of states (PDOS) shown in Figs.2(a)–2(b) illuminates that the triple $R'_{25}$ is mainly contributed by the p state of Li atoms and $X_2$ is mainly contributed by the s states of H atoms. The metallic behaviour from $LiBeH_3$ to $BeLiH_3$ induced by the inverse between Li and Be atoms comes from the lowering of the conduction bands $M_3$ and $R'_{25}$, and the increasing of the valence band $X_2$, which is mainly dominated by the moving of $M_3$. From Figs.2(a) and 2(c), it is known that the $M_3$ state is mainly contributed by the s states of the atoms located at the corner site, namely Li in $LiBeH_3$ and Be in $BeLiH_3$, and the $X_2$ state is mainly contributed by the s states of H atoms. Another obvious difference between $LiBeH_3$



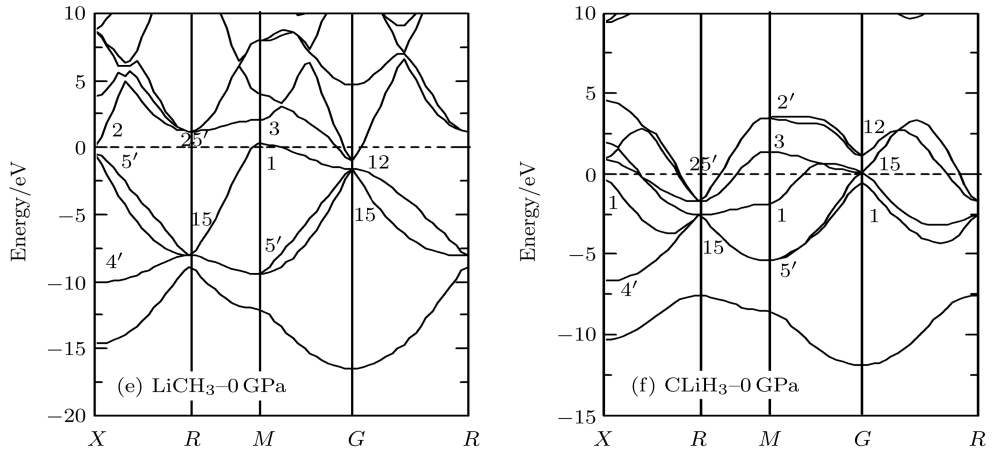
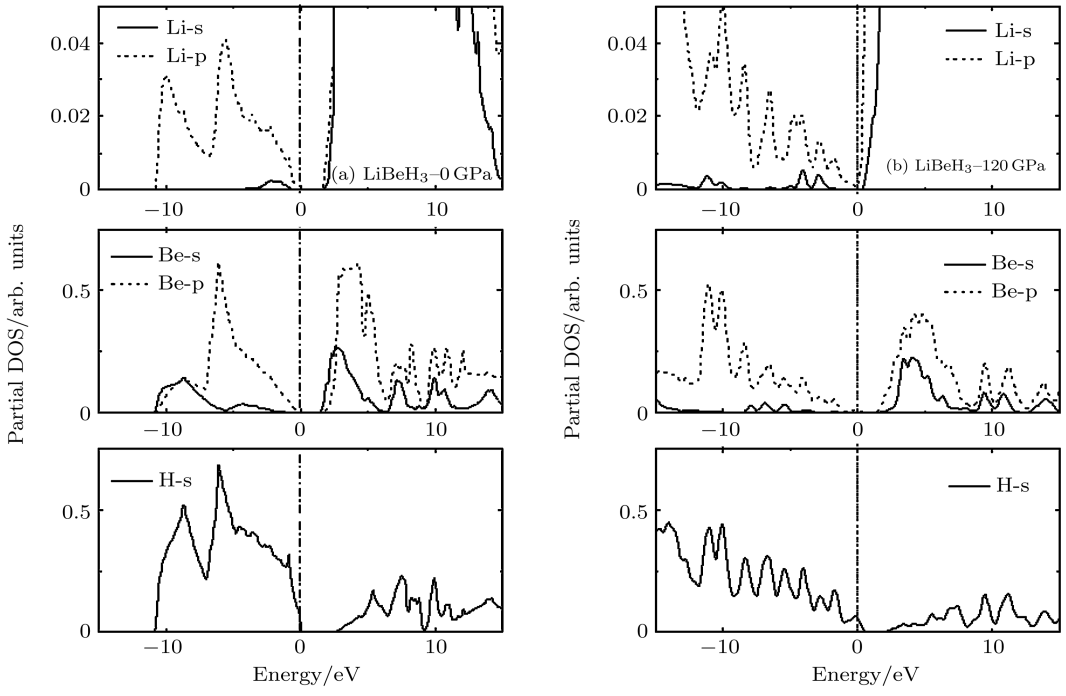



**Fig.1.** Calculated band structures of LiBeH$_3$ at 0 and 120 GPa, and of BeLiH$_3$, LiBH$_3$, LiCH$_3$, and CLiH$_3$ at 0 GPa, separately. The dashed line indicates the Fermi level.

and BeLiH$_3$ is the energy splittings of $X_1$ and $X_4'$, which are also found in Ref.[6]. In BeLiH$_3$, the valence band at $X_1$ is raised in energy due to the antibonding between Li-p and Be-s orbitals, and the hybridization among Li-p, Be-p and H-s states turns stronger.

The metallic behaviours from LiBeH$_3$ to LiBH$_3$ induced by increasing the electronegativity of the host matrix come mainly from the lowering of the conduction bands $R_1$ and $G_{15}$. As shown in Figs.2(a) and 2(d), the $R_1$ state is mainly contributed by the s states of Be or B atom. In LiBH$_3$, the conduction band at $R_1$ is lowered in energy because here B-s states bond with hydrogen states. In LiCH$_3$ and CLiH$_3$, shown in Figs.1(e) and 1(f), there is an isolated band in a lower energy range, which is possessed of ionic character due to the increasing of the hybridization among Li-p, C-s, p and H-s states. Especially in CLiH$_3$, C-s states and hydrogen states form electrovalent bonds. In LiCH$_3$ and CLiH$_3$, the metallic behaviours mainly come from the lowering of the conduction bands $G_{12}$ and $R_{25}'$, respectively. From Figs.2(e) and 2(f), it is known that the Fermi level of LiCH$_3$ is mainly dominated by C-p electrons, and that of CLiH$_3$ is mainly dominated by C-p and H-s electrons. Above all, from the PDOS, it is found that $X$-p electrons play an important role in the Fermi level of Li$X$H$_3$ hydrides having metallicity at 0 GPa, and H-s electrons play an important role in the Fermi level of $X$LiH$_3$ hydrides at 0 GPa. As for the Fermi level of LiBeH$_3$ at a metallization pressure of 120 GPa, it is dominated mainly by H-s electrons.



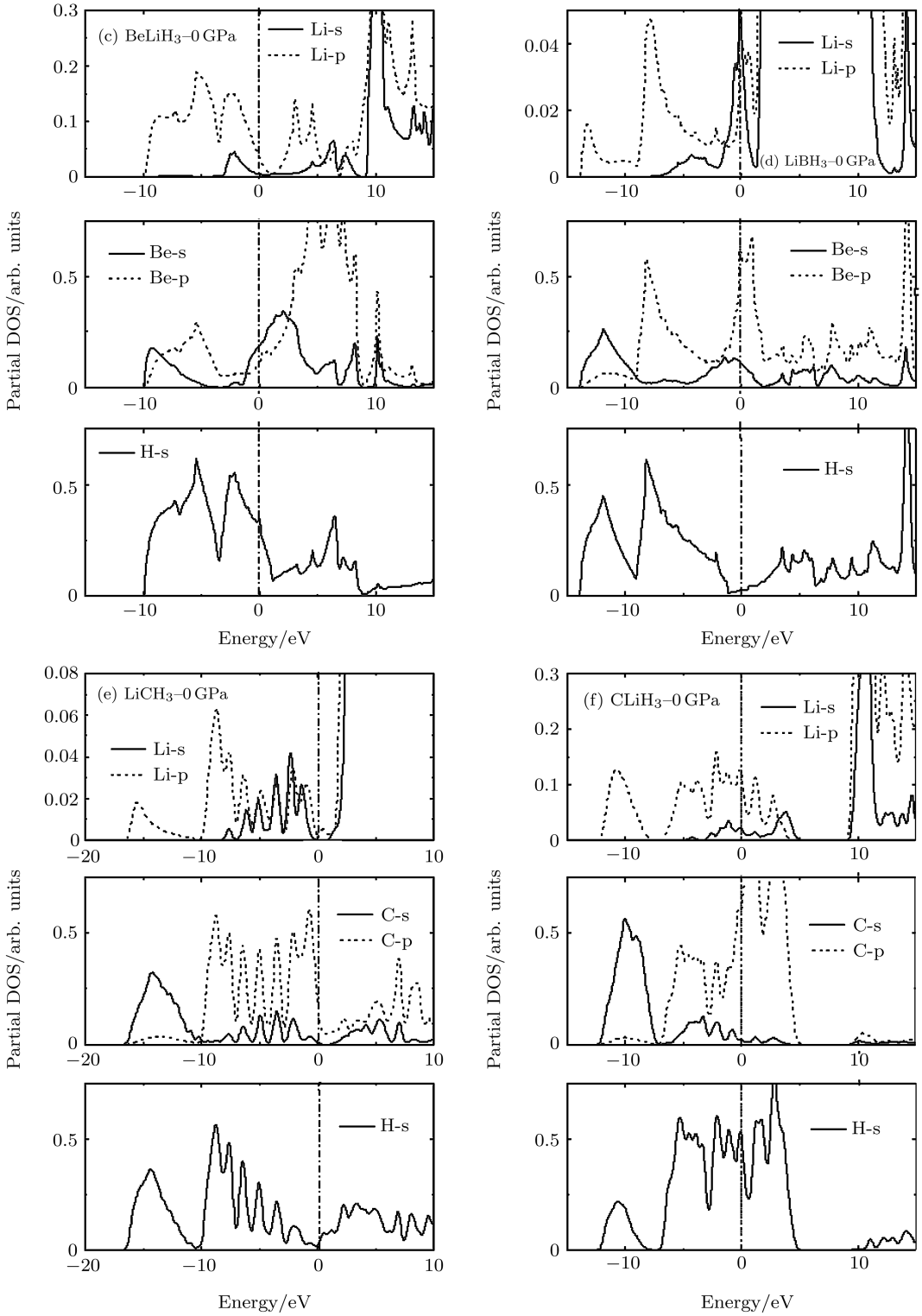



**Fig.2.** The calculated partial densities of states of $LiBeH_3$ at 0 and 120 GPa, and of $BeLiH_3$, $LiBH_3$, $LiCH_3$, and $CLiH_3$ at 0 GPa, respectively.

For understanding the difference in PDOS at Fermi level between $LiXH_3$ and $XLiH_3$, we analyse the redistribution of electronic configurations of all the investigated hydrides at 0 GPa shown in Fig.3(a). The results of $LiXH_3$ and $XLiH_3$ are plotted by using open symbols and a line with solid symbols, respectively. The negative value represents electropositivity, indicating the decrease of electrons due to the for-

mation of hydrides, and the positive one represents electronegativity, indicating the increase of electrons.

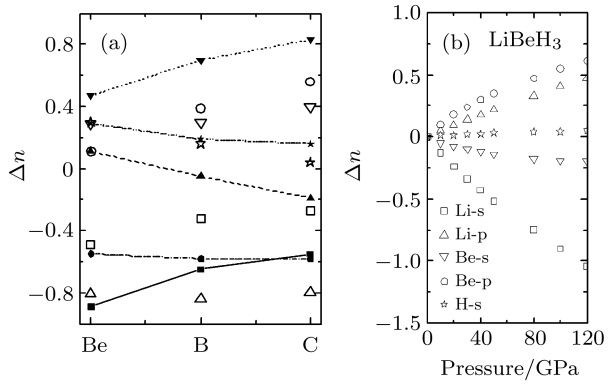



**Fig.3.** The redistribution of electronic configurations of all the investigated hydrides at 0 GPa (a) and the pressure effect on LiBeH$_3$ (b), with open symbols and line with solid symbol denoting. Li$X$H$_3$ and $X$LiH$_3$ represented, and squares, up-triangles, down-triangles, circles, and pentacles representing the Li-s, Li-p, $X$-s, $X$-p, and H-1s, respectively.

From Fig.3(a), it is clearly seen that the electronegativities of $X$-s and $X$-p in the series of Li$X$H$_3$ hydrides increase with the increase of atomic number $X$, especially the electronegativity of $X$-p electrons, but only the electronegativity of $X$-s in the series of $X$LiH$_3$ hydrides increases. The electronegativities of H-s in Li$X$H$_3$ and $X$LiH$_3$ hydrides decrease with the increase of atomic number $X$. Both $X$-p and Li-p electrons show different behaviours due to the exchange between Li and $X$ atoms, e.g. $X$-p electrons have an electronegativity and Li-p has a large electropositivity in Li$X$H$_3$ hydrides, but $X$-p electrons have an electropositivity in $X$LiH$_3$ hydrides which does not change merely with the increase of $X$ atomic number. The Li-p in BeLiH$_3$ has an electronegativity, but those in BLiH$_3$ and CLiH$_3$ have a slight electropositivity. From Fig.3(a), it is found that the electronegativity of $X$-p electrons is responsible for the metallicity of the investigated Li$X$H$_3$ hydrides, but the electronegativity of $X$-s electrons plays an important role in the metallicity of the investigated $X$LiH$_3$ hydrides. Furthermore, there occurs an electron transfer from $X$-p to $X$-s due to the formation of hydrides in $X$LiH$_3$, which lowers the host Fermi level and makes the hydrogen-related bands lie close to the Fermi level. It is clear that the metallization from LiBeH$_3$ to BeLiH$_3$ is induced by the increase of the electronegativity of Be-s electrons.

The pressure effect on the redistribution of electronic configurations in LiBeH$_3$ is shown in Fig.3(b). At 0 GPa, the electronegativity of H-s electrons is the largest one in the host matrix of LiBeH$_3$, so the hydrogen-related levels lie closest to the Fermi level. There appear electron transfers from Li-s to Li-p, Be-p and H-s orbitals, and from Be-s to Be-p orbitals in LiBeH$_3$ with the increase of pressure. Such an electron transfer increases the electronegativities of Be-p and H-s, but decreases the electronegativity of Be-s. Owing to the decrease of the electronegativity of Be-s, the total electronegativity of Be atom increases slowly with pressure. But the electronegativity of the host atom Be is more significant under higher pressures, which makes the hydrogen-related bands lie closer to the Fermi level. Above all, we believe that the increase of Be-p electrons with pressure plays an important role in the pressure-induced metallization in LiBeH$_3$.

In order to further understand the investigated hydrides, we investigate the optical properties. The imaginary parts of directionally averaged dielectric function $\varepsilon_2(\omega)$ of LiBeH$_3$ at 0 and 120 GPa and those of BeLiH$_3$, LiBH$_3$, LiCH$_3$, and CLiH$_3$ at 0 GPa are shown in Figs.4(a)–4(f), respectively. In our calculations, the intraband excitation contribution to the optical properties is not included, which affects mainly the low energy infrared part of the spectra.

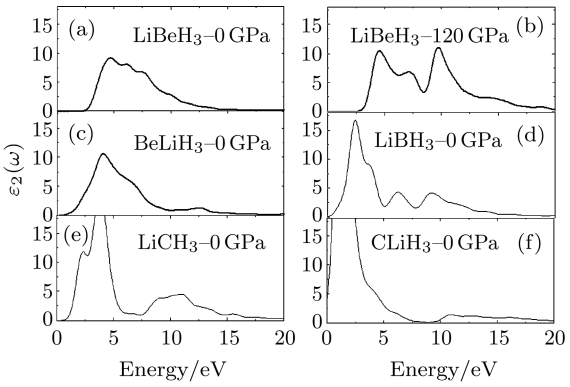



**Fig.4.** The calculated imaginary parts of the directionally averaged dielectric functions of LiBeH$_3$ at 0 and 120 GPa, and of BeLiH$_3$, LiBH$_3$, LiCH$_3$, and CLiH$_3$ at 0 GPa, respectively.

From Fig.4(a), one observes that the dielectric function of LiBeH$_3$ increases steeply above 2.5 eV and the peak is just located at about 4.7 eV. The spectrum of LiBeH$_3$ has three shoulders in a range from 5.0 to 10.0 eV. These features in dielectric function can be directly linked to the transitions from $X_2$ to $X_5'$, from $R_{15}$ to $R_1$, and from $R_{15}$ to $R_{25}'$, respectively. With pressure increasing, there is a clean-cut structure in the $\varepsilon_2(\omega)$ of LiBeH$_3$ above 8.0 eV as shown in Fig.4(b),

which makes the spectrum have two main peaks at about 5.0 and 10.0 eV, and two shoulders just above the two peaks, respectively. The spectrum of $BeLiH_3$ shown in Fig.4(c) is qualitatively different as it rises at 0 eV and has a strong peak at about 4.0 eV with a broad shoulder above it. Furthermore, there is a minor peak at a photon energy of 12.0 eV. Figure 4(d) shows that the substitution of B atom for Be atom results in a large shift of the dielectric response to lower energies, which can be related to the disappearance of the peak at the bottom of the conduction band $R_1$ with s characters of B atom. The transitions at $X_2$ that become allowed result in a peak in the dielectric function at about 2.4 eV. There are two clean-cut structures in the $\varepsilon_2(\omega)$ of $LiBH_3$ at 5.0 and 7.8 eV, respectively, as shown by those in $LiBeH_3$ under high pressures. Since the bands of H in $LiBH_3$ have a larger dispersion than those in $LiBeH_3$, its optical response spreads out over a larger energy range. In the case of $LiCH_3$ shown in Fig.4(e), there are two main peaks at about 4.0 and 10.0 eV, separately, and the first peak has a left-shoulder at about 2.2 eV. In the spectrum of $CLiH_3$ shown in Fig.4(f), the dielectric function has a sharper peak at about 1.5 eV than those of the other investigated hydrides.

From Fig. 4, it is clear that the optical responses of $LiBeH_3$ and $BeLiH_3$ are qualitatively similar despite considerable differences between their electronic structures and between band gaps. However, the optical absorption of other investigated hydrides has a much stronger and steeper peak in a lower energy range than those of $LiBeH_3$ and $BeLiH_3$, especially in the case of $CLiH_3$. These optical results are useful for understanding synthesizing and measuring these hydrides.

# 4. Conclusions

The equilibrium lattice constant, the cohesive energy and the electron properties of light metal hydrides with perovskite lattice structures have been investigated by using the pseudopotential plane-wave method. Large gap of $LiBeH_3$ indicates that it is insulating, but other investigated hydrides are all metallic. In particular, our results show that the pressure-induced metallization of $LiBeH_3$ could occur at about 120 GPa, which is induced mainly by the increase of Be-p electrons with the increase of pressure. We also find that the electronegativity of $X$-p electrons is responsible for the metallicity of the investigated $LiXH_3$ hydrides, but the electronegativity of $X$-s electrons plays an important role in the metallicity of the investigated $XLiH_3$ hydrides. Furthermore, in a series of $XLiH_3$ hydrides, there is an electron transfer from $X$-p to $X$-s due to the formation of hydrides, which lowers the host Fermi level and makes the hydrogen-related levels lie close to it. Therefore, the metallization from $LiBeH_3$ to $BeLiH_3$ is induced by the increase of the electronegativity of Be-*s* electrons. We have studied the dielectric functions of the series of hydrides. The optical absorptions of both $LiBeH_3$ and $BeLiH_3$ have a strong peak at about 5 eV and their optical responses are qualitatively similar. However, the optical absorptions of other investigated hydrides are much stronger than those of $LiBeH_3$ and $BeLiH_3$ in lower energy ranges, especially in the case of $CLiH_3$.

# References


[1] Overhauser A W 1987 *Phys. Rev.* B **35** 411
[2] Overhauser A W 1987 *Int. J. Mod. Phys.* B **1** 927
[3] Martins J L 1988 *Am. Phys. Soc.* **33** 709
[4] Martins J L 1988 *Phys. Rev.* B **12** 776
[5] Gupta M and Percheron-Guegan A 1987 *J. Phys.* F: *Met. Phys.* **17** L201
[6] Yu R and Lam P K 1988 *Phys. Rev.* B **38** 3576
[7] Seel M, Kunz A B and Hill S 1989 *Phys. Rev.* B **39** 7949
[8] Khowash P K, Rao B K, McMullen T and Jena P 1997 *Phys. Rev.* B **55** 1454
[9] Bell N A and Coates G E 1968 *J. Chem. Soc.* (A) **1968** 628
[10] Souw V, Li S, Metcalf P and McElfresh M 2002 *Phys. Rev.* B **65** 094510
[11] Shi D H, Liu Y F, Sun J F, Yang X D and Zhu Z L 2006 *Chin. Phys.* **15** 1015
[12] Shi D H, Liu Y F, Sun J F, Zhu Z L and Yang X D 2006 *Chin. Phys.* **15** 2928
[13] van Setten M J, Popa V A, de Wijs G A and Brocks G 2007 *Phys. Rev.* B **75** 035204
[14] Singh D J 1994 *Planewaves, Pseudopotentials and the LAPW Method* (Boston: Kluwer) p6
[15] Segall M D, Lindan P J D, Probert M J, Pickard C J, Hasnip P J, Clark S J and Payne M C 2002 *J. Phys.: Condens. Matter* **14** 2717
[16] Perdew J P, Burke K and Ernzerhof M 1996 *Phys. Rev. Lett.* **77** 3865
[17] Vanderbilt D 1990 *Phys. Rev.* B **41** 7892
[18] Monkhorst H J and Pack J D 1976 *Phys. Rev.* B **13** 5188
[19] Pack J P and Monkhorst H J 1977 *Phys. Rev.* B **16** 1748
[20] Fischer T H and Almlof J 1992 *J. Phys. Chem.* **96** 9768
[21] Bouckaert L P, Smoluchowski R and Wigner 1936 *Phys. Rev.* **50** 58